machines

Article

Solution of Spatial Transformation Relationship of Similar Ruled Surfaces Based on Registration of Divided Regions

Feiyan Han *, Zhitao Hu, Longlong He, Xianlong Peng, Manzhi Yang and Chuanwei Zhang

School of Mechanical Engineering, Xi'an University of Science and Technology, Xi'an 710000, China
* Correspondence: hfy@xust.edu.cn

Abstract: Since the geometric transformation relationship of similar surfaces with complex features, such as local deformation and curvature changes, is hard to be solved through global registration, this paper proposes a method for solving the spatial transformation relationship of similar ruled surfaces based on registration of divided regions. First, an adaptive region division algorithm is proposed to divide similar surfaces, and then, an improved registration algorithm is proposed by adding two constraints which are the curvature feature and differential geometric features of point clouds. Through this improved registration algorithm, the geometric transformation relationship of each sub-region can be solved, and then the spatial geometric transformation relationship of the overall similar surface can be established. Moreover, the improved registration algorithm can ensure that the differential geometric properties of corresponding points are similar after registration, which may provide a basis for mapping and reuse of process knowledge between corresponding points on similar surfaces. Finally, two similar ruled surface blades are taken as examples for simulation verification, the results show that the maximum registration error of each sub-region is 0.025 mm, which is within the allowable error range, and the registration speed of the proposed algorithm is better than the S-ICP algorithm. This proves that the method in this paper is feasible and effective.

Keywords: region division; scaling registration; spatial transformation relationship; similar ruled surfaces

Citation: Han, F.; Hu, Z.; He, L.; Peng, X.; Yang, M.; Zhang, C. Solution of Spatial Transformation Relationship of Similar Ruled Surfaces Based on Registration of Divided Regions. *Machines* **2022**, *10*, 956. https://doi.org/10.3390/machines10100956

Academic Editor: Kai Cheng

Received: 14 September 2022
Accepted: 18 October 2022
Published: 19 October 2022

1. Introduction

The current research on the reuse of CNC (Computer Numerical Control) machining processes focuses on searching for similar processes or similar cases in the database or instance library according to the similarity of the geometric shape or topological structure of the parts and realizing the reuse of process knowledge through inheritance or modification [1]. However, the above methods ignore the close relationship between the 3D geometry of the parts and the CNC machining process of process knowledge reuse [2], which leads to the mismatch between the reused similar process knowledge and the CNC machining process of similar parts. This situation is particularly serious on complex surfaces due to their complex shape and structure [3], the similar processing techniques such as machining methods; cutting conditions [4] and tool parameters [5] obtained through model retrieval [6] cannot be completely copied to the CNC machining of similar surface parts. Therefore, in order to accurately and effectively realize the reuse of process knowledge between similar free-form surface parts, after obtaining the similar process of free-form surface parts, it is important to study the internal mathematical relationship between similar free-form surface parts and reveal the spatial geometric transformation relationship between free-form surface parts; only by this way, the reuse of machining knowledge between similar free-form surface parts can be realized. At present, the spatial transformation relationship between similar surfaces is roughly divided into rigid transformation and non-rigid transformation. In order to solve the rigid transformation relationship between similar surfaces, Thompson et al. [7] transformed the transformation relationship between surfaces into a mathematical least square problem and obtained a rigid transformation matrix between surfaces through iterative method, but the obtained transformation matrix was not the optimal solution of the least square problem. In [8], Horn et al. proposed the quaternion method for the above problems, and successfully solved the problem of solving the rigid transformation matrix based on least-squares principle, but there are problems such as complex calculation and low precision. Besl and Mckay [9] proposed the iterative closest point (ICP) algorithm, which searches the nearest corresponding point on the point cloud of the two surfaces and matches it to obtain the transformation matrix. At present, it is still a widely used method to solve the surface transformation relationship. However, the algorithm has high requirements on the initial positions of the two surfaces, and it has a large amount of calculation, so many scholars have optimized and improved it. For example, Yao et al. [10] simplified point cloud data and improved registration efficiency by introducing curvature feature similarity into point cloud registration. Xu [11] and Li et al. [12] improved the ICP algorithm by combining the Random Sample Consistency (RANSAC) algorithm, so the problem of low accuracy and poor robustness when registering large point clouds by traditional methods were solved. However, when the point cloud has noise and low overlap rate, the point cloud registration result is difficult to guarantee [13]. Lu et al. [14] applied multiple constraints such as curvature and distance to the point cloud for accurate registration, which solved the registration problem of similar surfaces with low feature recognition. Yu et al. [15] proposed a new registration pipeline that focuses on object-level alignment, thus overcoming the difficulty of point cloud registration with low overlap rates. However, the above algorithms cannot solve the case that two surfaces have different scales. In order to solve the problem of non-rigid transformation between similar surfaces, Du et al. [16] put forward the S-ICP algorithm, this algorithm can register point clouds with different scales. Wang [17] and Shu et al. [18] proposed a multi-directional affine registration algorithm, which can register the 3D point cloud of multi-directional affine transformation, so as to solve the scale parameters between similar surfaces.

The solution methods for the above spatial transformation relationships are based on the idea of overall registration; however, when there are complex flexible transformations such as local deformation or overall curvature changes between similar surfaces, traditional registration algorithms cannot perform good registration of similar surfaces [19]. Therefore, in order to solve the spatial geometric transformation relationship between such similar surfaces, this paper proposes a method for solving the spatial transformation relationship based on registration of divided regions. Taking two similar ruled surface blade parts with complex transformation features as an example, first, the adaptive region division algorithm is used to segment similar surfaces. Before registering each sub-region, the point cloud is screened by the curvature similarity between the point pairs, and then the S-ICP algorithm is used for accurate registration to solve the geometric transformation relationship of each sub-region. Therefore, the overall spatial transformation relationship of similar surfaces can be established through the geometric transformation relationship of each sub-region. Finally, the local coordinate system of the point cloud is defined, and the point pairs after S-ICP registration are screened by imposing range constraints on the rotational deviation of the local coordinate system, so as to ensure that the differential geometric properties between the corresponding points are similar, it provides the possibility for the subsequent realization of the mapping and reuse of process knowledge between corresponding points.

2. Description of Spatial Transformation Relationship

If a surface can be transformed into another surface with similar geometric shape through scaling, rotation, and translation transformation, it can be described that the two surfaces are similar [20].This spatial transformation relationship can be called affine transformation, in which scaling transformation can be divided into uniform scaling and non-uniform scaling [21]. The scaling transformation matrix S can be represented by three scaling components s_x, s_y, and s_z of the coordinate axis as:

$$S = \begin{bmatrix} s_x & & \\ & s_y & \\ & & s_z \end{bmatrix} \tag{1}$$

where $s_x > 0, s_y > 0, s_z > 0$, when $s_x = s_y = s_z$ is uniform scaling.

The rotation matrix R is generally represented by three rotation variables α, β, γ around the three-coordinate axis, that is:

$$\begin{aligned} R &= R_z(\alpha) \cdot R_y(\beta) \cdot R_x(\gamma) \\ &= \begin{bmatrix} \cos\gamma & -\sin\gamma & 0 \\ \sin\gamma & \cos\gamma & 0 \\ 0 & 0 & 1 \end{bmatrix} \cdot \begin{bmatrix} \cos\beta & 0 & \sin\beta \\ 0 & 1 & 0 \\ -\sin\beta & 0 & \cos\beta \end{bmatrix} \cdot \begin{bmatrix} 1 & 0 & 0 \\ 0 & \cos\alpha & -\sin\alpha \\ 0 & \sin\alpha & \cos\alpha \end{bmatrix} \\ &= \begin{bmatrix} \cos\beta\cos\gamma & \sin\alpha\sin\beta\cos\gamma - \cos\alpha\sin\gamma & \cos\alpha\sin\beta\cos\gamma + \sin\alpha\sin\gamma \\ \cos\beta\sin\gamma & \sin\alpha\sin\beta\sin\gamma + \cos\alpha\cos\gamma & \cos\alpha\sin\beta\sin\gamma - \sin\alpha\cos\gamma \\ -\sin\beta & \sin\alpha\cos\beta & \cos\alpha\cos\beta \end{bmatrix} \end{aligned} \tag{2}$$

where $\alpha, \beta, \gamma \in (-\pi, \pi]$, $R_\Delta(\theta)$ is expressed as a rotation transformation matrix that rotates the θ angle counterclockwise around the Δ axis.

The translation vector T can be represented by the 3 translation components t_x, t_y, t_z along the coordinate axis as:

$$T = \begin{pmatrix} t_x \\ t_y \\ t_z \end{pmatrix} \tag{3}$$

It can be seen from the above that the spatial geometric transformation relationship between two similar surfaces can be established by three variables: scaling S, rotation R, and translation T. Supposing that the coordinate points (x, y, z) on the surface s are affine transformation into the coordinate points (x′, y′, z′) on the corresponding surface s′, the three-dimensional Euclidean space affine transformation can be obtained:

$$\begin{bmatrix} x' \\ y' \\ z' \end{bmatrix} = SR \begin{bmatrix} x \\ y \\ z \end{bmatrix} + T \tag{4}$$

Not all spatial transformation relationships of similar free-form surfaces can be expressed by the above affine transformation matrix. When there are local deformations, surface twists, and overall curvature changes between two similar surfaces, it is generally difficult to use a simple display function mapping relationship to represent the overall transformation relationship. Therefore, in order to solve the spatial transformation relationships of such similar surfaces, the whole surface is divided into several regions according to the curvature characteristics of the surface in this paper, and then each sub-region is registered to solve the spatial geometric transformation relationship m_i of each sub-region, so that the spatial geometric transformation relationship $m = \{m_1, m_2, m_3, \ldots, m_n\}$ of the entire similar surface can be established, which according to the geometric transformation relationship m_i of each sub-region.

3. Solving the Spatial Transformation Relation

The proposed method in this paper for solving the spatial transformation relationship of similar surfaces is divided into four parts: adaptive region division, curvature characteristic constraints, point cloud registration to solve transformation parameters, and local coordinate system constraints. The main idea is to use adaptive region division algorithm to segment similar surfaces that cannot be registered directly, and then each sub region is registered after region division. Before each sub region is registered, the wrong point pairs are preliminarily screened through curvature similarity judgment, and then the S-ICP algorithm is used to register the point cloud; the geometric transformation relationship of each sub-region can be solved. Therefore, the overall spatial transformation relationship of similar surfaces can be established through the transformation relationship of each sub-region. Finally, the point pairs after registration are further screened by constraining the rotational deviation of the local coordinate system between the corresponding points, so as to ensure that the differential geometric properties between the corresponding points are similar.

3.1. Adaptive Region Division Algorithm for Similar Surfaces

For the division of surfaces, the parameters of the surface should first be selected as the basis for division [22]. Because the curvature is independent of the position, size, and posture of the free-form surface, the curvature is selected as the parameter for the division of similar surfaces. However, due to the differences between similar surfaces such as local deformation and overall curvature inconsistency, the method of dividing the surface by the curvature of each point on the surface can only reflect the respective differential geometric properties of similar surfaces, so the corresponding regions between similar surfaces still have the problem of inconsistency in the size of curvature and degree of deformation, which leads to the registration effect is still unsatisfactory. Therefore, the curvature mutation points on the boundary are used to divide the surfaces in this paper, so as to better reflect the curvature characteristics on the surfaces. It can also ensure that the curvature characteristics of the corresponding sub regions after segmentation are as similar as possible, so as to achieve good registration between corresponding regions.

Given two similar surfaces P and P′, extract all feature points on the boundaries of surfaces P and P′, then record them as feature point sets $Z=\{\mathrm{z_i}|\mathrm{z}_i \in \mathrm{R}, \mathrm{i}=1,2,\ldots,\mathrm{n}\}$ and $Z'=\{\mathrm{z_j}\prime|\mathrm{z_j}\prime \in \mathrm{R}, \mathrm{j}=1,2,\ldots,\mathrm{m}\}$, respectively. Using the moving least squares method [23] to solve the maximum principal curvature $\mathrm{k}_1(z_i)$ and the minimum principal curvature $\mathrm{k}_2(\mathrm{z}_i)$ of each feature point z_i in the point sets Z, where $\mathrm{k}_1(\mathrm{z}_i)$ and $\mathrm{k}_2(\mathrm{z}_i)$ represent the maximum and minimum bending degrees at the feature point, respectively; therefore, the curvature characteristic parameter is defined as [24]:

$$\xi(\mathrm{z}_i) = \frac{1}{2} - \frac{1}{\pi}\mathrm{arctan}\frac{k_1(\mathrm{z}_i) + k_2(\mathrm{z}_i)}{k_1(\mathrm{z}_i) + k_2(\mathrm{z}_i)} \tag{5}$$

According to the definition of Equation (5), two criteria for judging whether z_i is characteristic point of curvature mutation are obtained:

$$\xi(\mathrm{z}_i) > \max[\xi(\mathrm{z}_{i,1}), \xi(\mathrm{z}_{i,2}), \ldots, \xi(\mathrm{z}_{i,\mathrm{j}})] \tag{6}$$

$$\xi(\mathrm{z}_i) < \min[\xi(\mathrm{z}_{i,1}), \xi(\mathrm{z}_{i,2}), \ldots, \xi(\mathrm{z}_{i,\mathrm{j}})] \tag{7}$$

where $\xi(\mathrm{z}_{i,\mathrm{j}})$ is the curvature characteristic parameter of the adjacent feature points of point z_i. If Equation (6) is satisfied, then z_i is considered as the boundary convex point; if Equation (7) is satisfied, then z_i is considered as the boundary concave point. If one of the two is satisfied, then z_i is regarded as the boundary curvature mutation point, and stored in the boundary curvature mutation pointset C, and record the u, v parameter values of each boundary curvature mutation point as $\{\mathrm{u}_{\mathrm{c}_i}, v_{c_i}\}$, where $\mathrm{u}, v \in [0,1]$. As shown in Figure 1a, the distribution of surface boundary curvature mutation point can reflect the local deformation of the surface and the change of the curvature. Therefore, the surface P can be divided by connecting the boundary points. However, due to the large number of curvature mutation points, it is necessary to select appropriate curvature mutation points to divide the surface. The principle of selection is that the characteristic points with similar u or v values on both sides of the surface, which are called "boundary points". As shown in Figure 1b, the red point is the final selected "boundary point", and the line connecting the boundary point is called the "boundary line". In order to ensure that the boundary line can reflect the curvature characteristics of the surface, and the region division can be better realized, the corresponding boundary points are connected by fitting curve in this paper. As shown in Figure 1c, because the u and v values of the corresponding boundary points at both ends of the surface are different, in order to make the boundary lines as smooth as possible, the isoparametric method is used to divide u direction or v direction in this paper, and then used the fit curve to connect the two corresponding boundary points to divide the surface. At the same time, in order to ensure that the regions between similar surfaces can be registered correspondingly, the number of sub regions divided by surface P and similar surface P′ should be consistent. Therefore, in the feature point sets Z', find the feature points with the same u, v parameter values as the points in the boundary curvature mutation points sets C, record them as the boundary curvature mutation points of the surface P′ and store them in the boundary curvature mutation points sets C′, then use them to divide the similar surface P′.

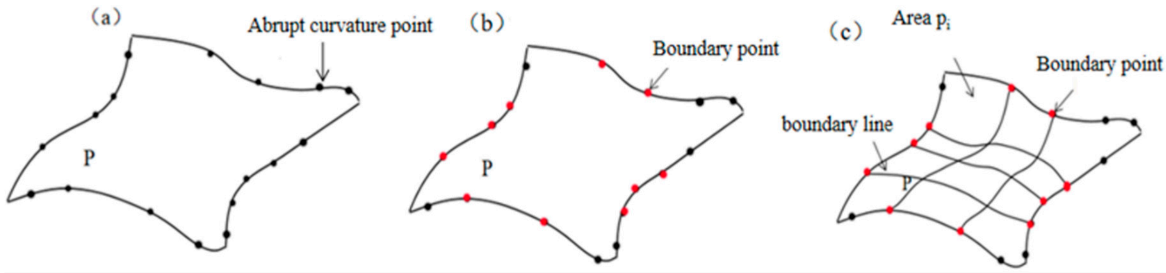

Figure 1. Selection of boundary points and region division of surfaces: (**a**) distribution of abrupt curvature points, (**b**) selection of boundary points, (**c**) surface region division.

From what is discussed above, the whole adaptive region partition algorithm is reasonably drawn out as follows.

Step 1. Extract all feature points on the boundaries of surfaces P and P′, then record them as feature point sets $Z = \{z_i | z_i \in R, i = 1, 2, \ldots, n\}$ and $Z' = \{z_j' | z_j' \in R, j = 1, 2, \ldots, m\}$, respectively.

Step 2. Compute $k_1(z_i)$ and $k_2(z_i)$ of each point in the point sets Z, and compute $\xi(z_i)$ according to Equation (5).

Step 3. Determine whether z_i is a boundary curvature mutation point by Equations (6) and (7), and store it in the boundary curvature mutation point sets C.

Step 4. Connect the boundary points to divide the surface *P* and output each division region $S_p = \{p_1, p_2, \ldots\ldots, p_n\}$.

Step 5. Establish the boundary curvature mutation point set C′ of the surface P′ according to the boundary curvature mutation point sets C, repeat the step to divide the surface P′, output each division region $S_{p'} = \{p_1', p_2', \ldots\ldots, p_n'\}$.

3.2. Similarity Judgment of Differential Geometric Properties

3.2.1. Curvature Property Constraints

Due to the high data density of the extracted similar surface point clouds, there may be a large number of redundant points, which seriously affects the efficiency of subsequent algorithms. Therefore, before registering point clouds, the number of point clouds should be screened according to certain requirements. Since curvature is a feature that does not change with translation, rotation, and scaling transformations, the point cloud can be preliminary screened by the curvature feature to remove the wrong point pairs.

Given two point sets $p_i = \{q_{p_i,x} | q_{p_i,x} \in R, x = 1, 2, \ldots, N\}$ and $p_i' = \{q_{p_i',y} | q_{p_i',y} \in R, y = 1, 2, \ldots, M\}$, which are the corresponding regional point sets in two similar surfaces, first, calculate the principal curvature $k_1(q_{p_i,x})$, $k_2(q_{p_i,x})$, and $k_1(q_{p_i',y})$, $k_2(q_{p_i',y})$ of each point in the point cloud sets p_i and p_i'. Then, for each point in the point set p_i, find the corresponding point with similar curvature characteristics in its corresponding point set $p_i\prime$. Therefore, the similarity judgment criterion of curvature is expressed as follows [25]:

$$\begin{cases} \frac{k_1(q_{p_i,x})-k_1(q_{p_i\prime,y})}{k_1(q_{p_i,x})+k_1(q_{p_i\prime,y})} < \alpha_1 \\ \frac{k_2(q_{p_i,x})-k_2(q_{p_i\prime,y})}{k_2(q_{p_i,x})+k_2(q_{p_i\prime,y})} < \alpha_2 \end{cases} \tag{8}$$

where α_1, α_2 are the curvature similarity thresholds, and only when the above two criteria are met, the curvature characteristics of point pairs are similar. Further, extract the point pairs that meet the judgment criteria of curvature similarity according to Equation (8), and store them in the corresponding point sets U_{p_i} and $U_{p_i\prime}$. The point cloud registration of each corresponding point set U_{p_i} and $U_{p_i\prime}$ is carried out through the S-ICP algorithm, so as the geometric transformation relationship $m_i = \{S_i, R_i, T_i\}, i = 1, 2, \ldots, n$ between each corresponding region can be solved.

3.2.2. Local Coordinate System Property Constraints

Whether the differential geometric properties of corresponding points between similar surfaces are similar is the basis for realizing process knowledge mapping and reuse between corresponding points, screening only by the curvature property of the corresponding points does not guarantee that the differential geometric properties of the corresponding points after registration are similar. Therefore, it is necessary to further screen the corresponding points after registration, and the normal vector and the tangent vector are important attributes to measure whether the differential geometric properties of corresponding points are similar. However, if only one of these variables is used to filter the point cloud, a point may have many corresponding points with similar differential geometric characteristics. Therefore, the normal vector, tangent vector and their vector product are combined to build the local coordinate system of the point cloud in this paper, and the corresponding points after S-ICP registration are further screened to ensure that the differential geometric properties between the corresponding points are similar.

Suppose O_u is any point in the corresponding point cloud set U_{p_i}, e_x is the unit normal vector of the point, e_y is the unit tangent vector, so its vector product is $e_z = e_x \times e_y$. As shown in Figure 2a, take O_u as the origin of the coordinate, and let the directions of e_x, e_y, e_z be the x_u, y_u, z_u axes, respectively, to establish the local coordinate system $O_u - x_u y_u z_u$ of the point. Similarly, construct the local coordinate system $O_{u\prime} - x_{u\prime} y_{u\prime} z_{u\prime}$ of its corresponding point $O_{u\prime}$ in the corresponding point set $U_{p_i\prime}$, where F_i is the tangent plane of the point. As shown in Figure 2b, in order to facilitate the observation of the rotation deviation of each axis of the corresponding point, the corresponding point is converted to the same coordinate system, so the rotation deviation angle $\theta_1, \theta_2, \theta_3$ of the normal vector, tangent vector, and vector product between the corresponding points can be calculated by Equation (9):

$$\cos\theta_i = \frac{\vec{a} \cdot \vec{b}}{|\vec{a}| \cdot |\vec{b}|}, \theta_i = \arccos\left(\frac{\vec{a} \cdot \vec{b}}{|\vec{a}| \cdot |\vec{b}|}\right) \tag{9}$$

Point pairs are further matched by changing the minimum distance measure between corresponding points to the minimum included angle measure. First, constraints are imposed on the rotational deviation of each axis, and then a weight factor is introduced to give different weights to the rotational deviations of each axis to further constrain the sum of the rotational deviations of the overall local coordinate system, so as to screen out the corresponding points with similar differential geometry. Since the normal vector can be used to describe the direction of the local surface and is an important feature of the surface geometry [26], it is necessary to ensure that the weight of the normal vector is relatively large. Therefore, the rotational deviation measurement formula of the local coordinate system given in this paper is as follows:

$$\omega = \omega(\theta_1, \theta_2, \theta_3) = \begin{cases} \theta_1 \le \delta_1 \\ \theta_2 \le \delta_2 \\ \theta_3 \le \delta_3 \\ \left(\frac{1}{2}\theta_1 + \frac{1}{4}\theta_2 + \frac{1}{4}\theta_3\right) \le \delta_4 \end{cases} \tag{10}$$

where δ_{i} is the rotational deviation threshold, and the point pairs that satisfy the constraints of each axis in Equation (10) at the same time are extracted to form the corresponding point sets with similar differential geometric properties. This method can effectively filter out the corresponding points with dissimilar differential geometric characteristics in the corresponding point clouds after registration. It provides the possibility of reusing machining process knowledge between corresponding points of similar surfaces.

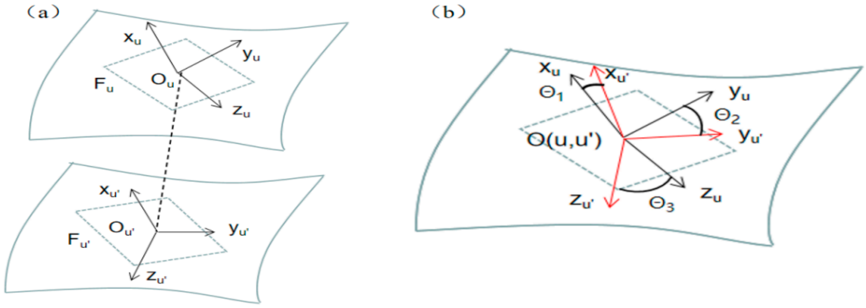

Figure 2. Local coordinate system and rotational deviation of corresponding points: (**a**) the local coordinate system of the corresponding point, (**b**) rotational deviation of the local coordinate system.

3.3. Region Registration Algorithm for Similar Surfaces

As shown in Figure 3, the point cloud registration algorithm based on region division can be reasonably obtained from the above discussion:

Step 1. Use the adaptive region division algorithm to segment similar surfaces, and denote the divided regions as $S_{\mathrm{p}} = \{\mathrm{p}_1, \mathrm{p}_2, \ldots\ldots, \mathrm{p}_{\mathrm{n}}\}$ and $S_{\mathrm{p}'} = \{\mathrm{p}_1{'}, \mathrm{p}_2{'}, \ldots\ldots, \mathrm{p}_{\mathrm{n}}{'}\}$

Step 2. Randomly select a regional point cloud sets $\mathrm{p}_i = \{\mathrm{q}_{\mathrm{p}_i,\mathrm{x}} | \mathrm{q}_{\mathrm{p}_i,\mathrm{x}} \in \mathrm{R}, \mathrm{x} = 1, 2, \ldots, \mathrm{N}\}$ from S_P, and select its corresponding regional point cloud sets $\mathrm{p_i}' = \{\mathrm{q}_{\mathrm{p_i}',\mathrm{y}} | \mathrm{q}_{\mathrm{p}_i',\mathrm{y}} \in \mathrm{R}, \mathrm{y} = 1, 2, \ldots, \mathrm{M}\}$ in $S_{P'}$.

Step 3. Calculate the principal curvature of each point in the point cloud sets $\mathrm{p_i}$ and $\mathrm{p_i}'$.

Step 4. Extract point pairs with similar curvature characteristics by Equation (8) and store them in corresponding point sets $U_{\mathrm{p_i}}$ and $U_{\mathrm{p_i}'}$.

Step 5. Input $U_{\mathrm{p_i}}$ and $U_{\mathrm{p_i}'}$, and solve the geometric transformation parameter $\mathrm{m_i} = \{\mathrm{S}_i, \mathrm{R}_i, \mathrm{T}_i\}$ of this region by S-ICP algorithm.

Step 6. The point pairs after registration are further filtered by Formula (10) to extract corresponding points with similar differential geometric characteristics.

Step 7. Repeat steps 3–7 for point sets $\mathrm{p_i}$ and $\mathrm{p_i}'$ in other regions to solve the m_i of each sub-region.

Step 8. the overall spatial transformation relationship $M = \{\mathrm{m}_1, \mathrm{m}_2, \mathrm{m}_3, \ldots, \mathrm{m}_n\}$ of similar surfaces can be established.

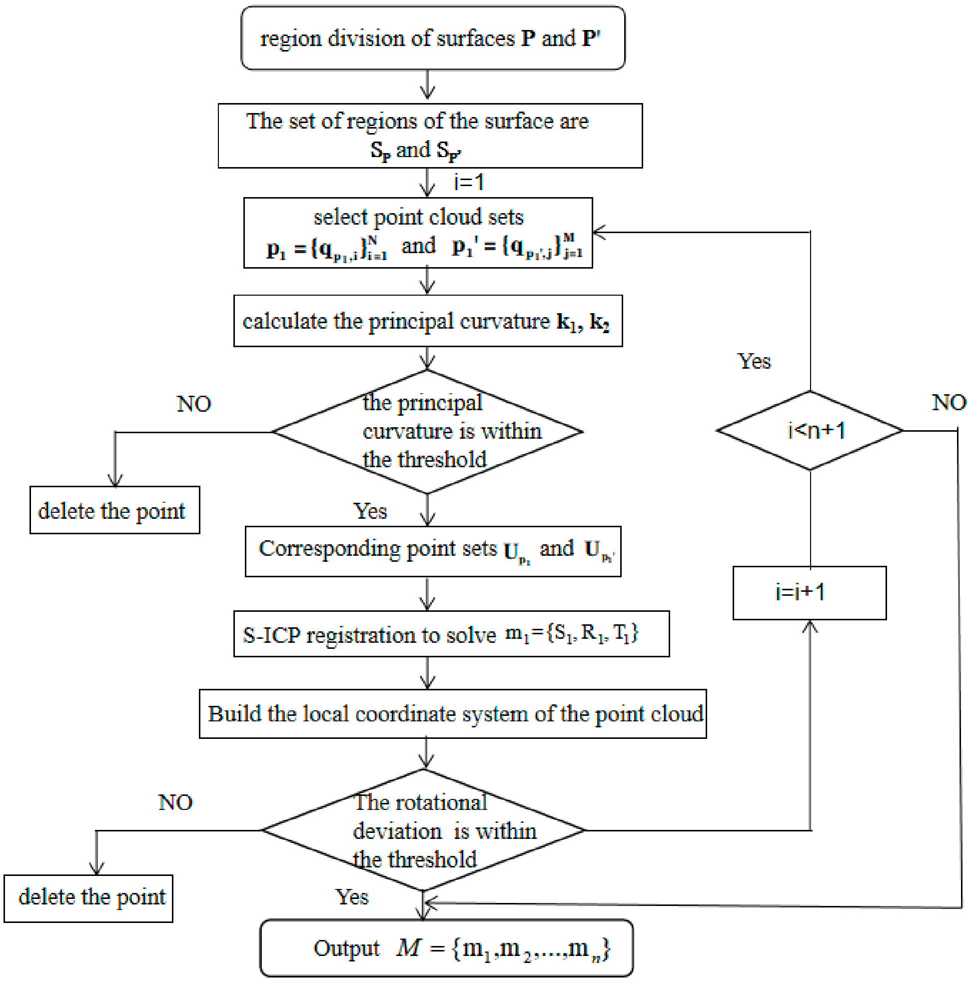

Figure 3. Flow chart of algorithm.

4. Experimental Design and Results

To prove the feasibility and effectiveness of the method proposed in this paper, similar blades of ruled surface were used for registration verification. The simulation was based on MATLAB 2020a, whose environment was configured for a 3.3 GHz CPU with 8 GB RAM. The root mean square error (RMSE) is applied to evaluate the error of the registration, the RMSE can be expressed as [16]:

$$RMS = \left(\frac{1}{\mathrm{N}} \sum_{\mathrm{x}=1}^{N} \left\| SRq_{p_{i,\mathrm{x}}} + T - q_{p\prime_i, c_k(\mathrm{x})} \right\|_2^2 \right)^{\frac{1}{2}} \tag{11}$$

4.1. Similar Surface Region Division

Figure 4 shows an example of two similar ruled surface blades P and P′ for comparative analysis. The length and width of blade P are 107.06 mm and 68.67 mm, respectively. The length and width of blade P′ are 79.42 mm and 53.27 mm, respectively. Blade P′ is the complex flexible transformation blade of P. The upper left position of the two blades shown in Figure 4a has significant bending deformation, and the overall curvature of the two blades shown in Figure 4b,c is obviously different. Therefore, it can be proven that the two similar blades selected in this paper have complex flexible transformation.

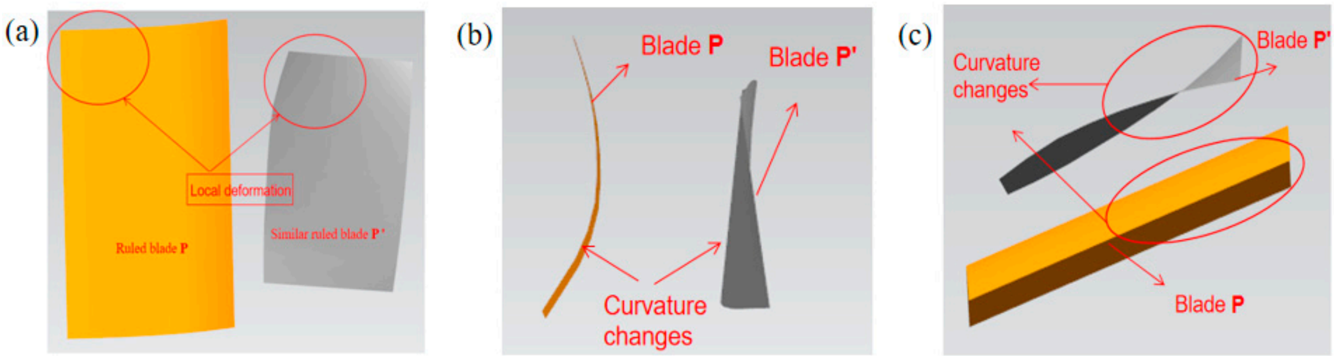

Figure 4. Three-dimensional model of two similar blades: (**a**) local deformation of similar blades, (**b**) vertical view of similar blades, (**c**) side view of similar blades.

The initial state of the point cloud model of two similar blades is shown in Figure 5a, and the results by applying the traditional registration method is shown in Figure 5b. It can be obvious seen that although the registration of blade on size is correct, the overall surface registration is still poor. This is because the registration accuracy of traditional methods is affected by the overall curvature and local deformation of the blades, and the greater the difference of blade, the lower the accuracy of registration. Therefore, the traditional global registration method is difficult to solve the registration problem of similar surfaces obtained from complex flexible transformations.

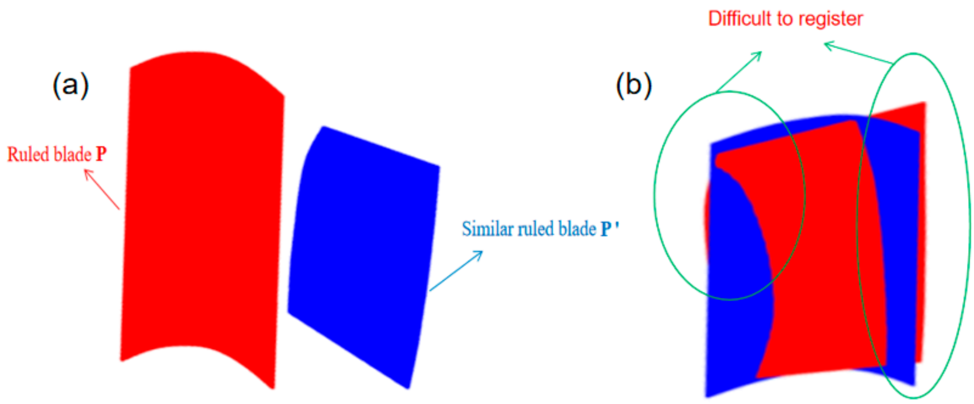

Figure 5. Overall point cloud registration of similar surfaces: (**a**) Point cloud initial state, (**b**) point cloud overall registration effect.

In order to solve the above-mentioned phenomenon of poor registration, an adaptive region division algorithm is proposed in this paper for region division of similar surfaces. As show in Figure 6a, first, the abrupt curvature points of the surface boundary were found through the algorithm; it can be seen that the abrupt curvature points are distributed at the obvious curvature change of the surface boundary, which can closely reflect curvature changes and local deformation. Then, the curvature mutation points with approximate u or v values on both sides of the blade as the boundary points were selected, as shown in Figure 6b; the red abrupt curvature points are called the boundary points. Finally, the fitting curve was used to connect the corresponding boundary points to complete the region division of blade P′. It can be seen from Figure 6c that the adaptive region division algorithm can achieve a good segmentation effect for the local deformation and obvious curvature changes of blade P′.

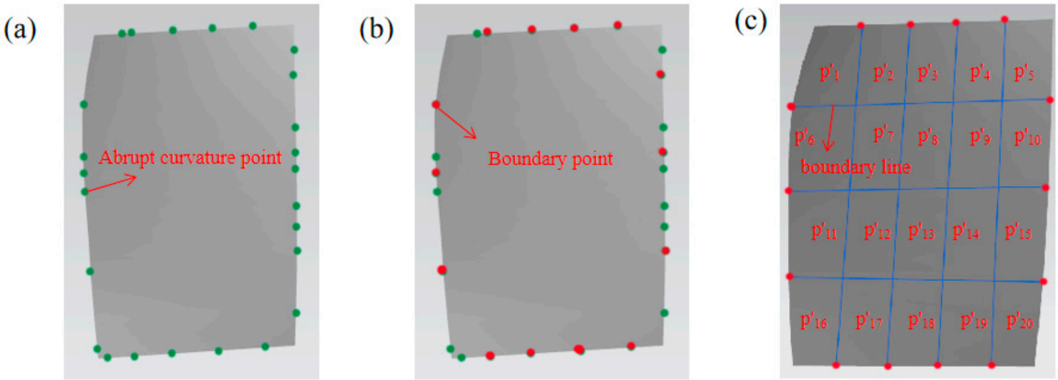

Figure 6. Region division of ruled blade P′: (**a**) distribution of abrupt curvature points, (**b**) extract boundary points for region division, (**c**) region division of blade.

After the blade P′ completes the region division, the adaptive region division algorithm is used to divide the region of blade P, and the result is shown in Figure 7. the boundary point on blade P has the same value of u and v parameters as the boundary points on blade P′. It can be seen that blade P is also divided into 20 sub regions. The shape and curvature of the corresponding sub regions of blade P and P′ are relatively similar, which provides a good initial condition for accurate registration between the corresponding regions.

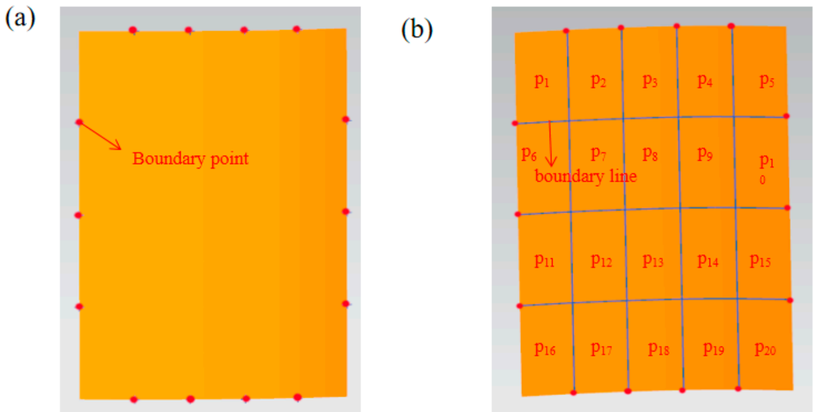

Figure 7. Region division of ruled blade P: (**a**) distribution of boundary points, (**b**) region division of blade.

4.2. Point Cloud Registration for Each Sub-Region

After each sub-region is divided, the S-ICP algorithm is used to register the point cloud of each sub-region to solve the geometric transformation relationship, and the corresponding regions p1 and p1′ are taken as examples in this paper. The registration result is shown in Figure 8a; it can be seen that the registration results of the divided regions are greatly improved compared with the overall registration results, and a good registration effect can be basically achieved. However, because point pairs with dissimilar curvature characteristics and differential geometric properties are not screened, there are many point pairs with inconsistent curvature at the diagonal positions that cannot be completely coincident, and there are also many corresponding points at the edges with different differential geometric properties. Figure 8b shows the registration result of the algorithm in this paper, due to the curvature characteristics and differential geometric properties of point pairs have been filtered, it can be seen from the figure that the registration effect of the method in this paper is generally better than the S-ICP algorithm, the areas that cannot be fitted due to inconsistent curvature become smaller, and the point pairs with dissimilar differential geometric properties at the edge of the surface are significantly reduced.

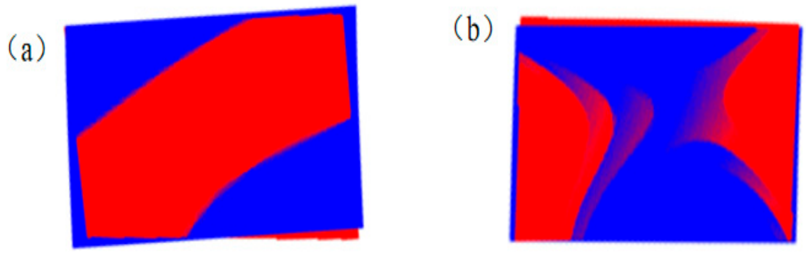

Figure 8. Point cloud registration effect comparison: (**a**) S-ICP algorithm, (**b**) region-registration algorithm.

It can be seen from Table 1 that the geometric transformation parameters between regions solved by the two methods are relatively close, the registration time of the method in this paper is reduced from 40.7 s to 30.5 s compared with the S-ICP algorithm, and the root mean square error is also reduced. This shows that this paper provides a good initial environment for precise registration by screening point pairs with large differences in curvature characteristics, which can effectively reduce the registration time and improve registration accuracy. At the same time, the differential geometric properties of the corresponding points can be ensured to be similar after the differential geometric properties of the point pairs are screened.

Table 1. Comparing the registration results of the two methods.

Method	Scale	Rotation	Translation	Time/s	RMES/mm
S-ICP algorithm	diag(0.753,0.766,0.754)	$\begin{matrix} 0.9674 & 0.0418 & 0.2498 \\ 0.0530 & 0.9309 & -0.3613 \\ -0.2477 & 0.3646 & 0.8984 \end{matrix}$	(29.22,20.86,92.10)	40.7	0.0564
Region-registration algorithm	diag(0.752,0.762,0.751)	$\begin{matrix} 0.9796 & -0.0540 & 0.1958 \\ 0.1206 & 0.9284 & -0.3482 \\ -0.1632 & 0.3646 & 0.9167 \end{matrix}$	(29.67,20.63,92.22)	30.5	0.0354

Figure 9 shows the registration results of the algorithm in this paper for each subregion between similar surfaces. It can be seen that the registration effect of each region is good, and there is no result that cannot be registered due to local deformation and curvature difference between regions. Even in the p_1 area with the largest bending deformation, the overall registration effect is still good except for a few edges that cannot be fitted, this also proves the effectiveness of the algorithm in this paper.

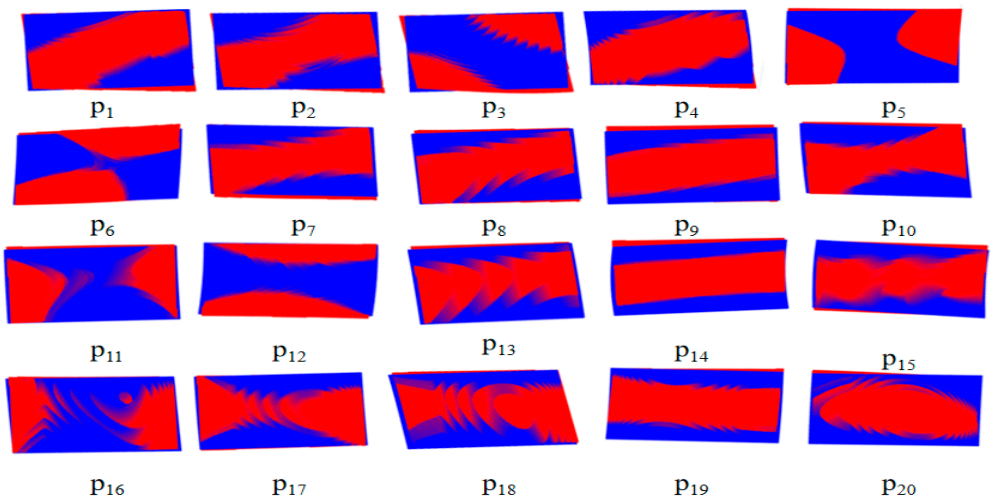

Figure 9. Point cloud registration for each sub-region.

The registration time and RMSE of the two methods for each sub-region are shown in Figures 10 and 11. It can be seen from the figure that the maximum RMSE of each region registered by the algorithm in this paper is 2.52×10^{-2}mm, and the RMSE of other regions fluctuates in 5×10^{-3}mm.The actual registration errors are all within the allowable error range $\sigma \leq 0.1$mm, this indirectly indicates that the geometric transformation relationship of each corresponding region solved by the method in this paper is relatively accurate. At the same time, since the reduction of the number of point pairs by screening out some wrong point pairs, the registration time of the method in this paper is significantly reduced compared with the SICP algorithm. Moreover, because point pairs with large differences in curvature characteristics and differential geometric properties are filtered out, the RMSE is also reduced.

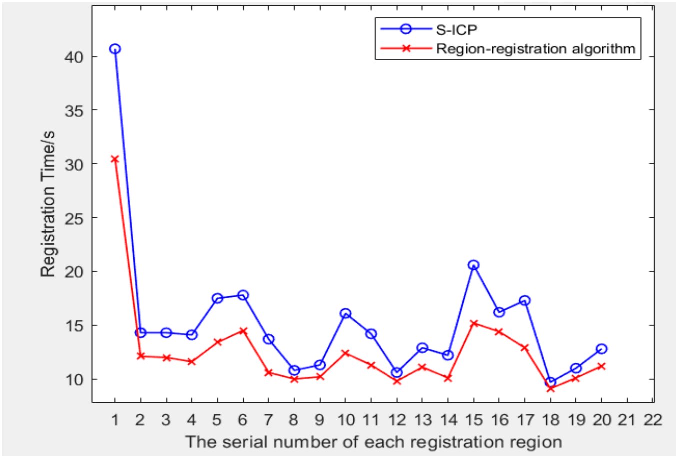

Figure 10. Registration time of each sub-region under two algorithms.

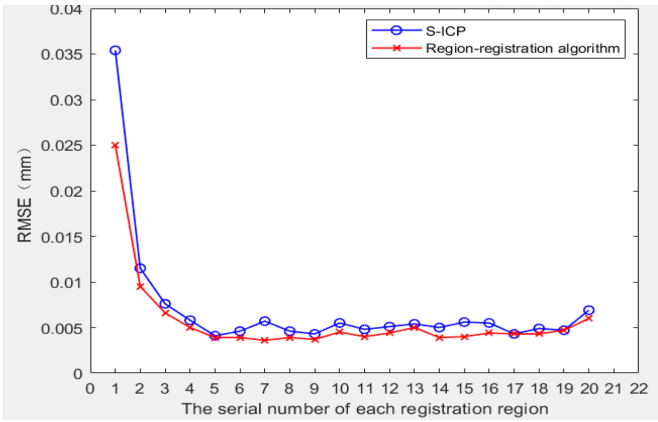

Figure 11. RMSE of each sub-region under two algorithms.

As shown in Figure 12, in order to verify that the overall spatial transformation relationship $M = \{m_1, m_2, m_3, \ldots, m_{20}\}$ of similar surfaces can be established by solving the geometric transformation relationship m_i of each sub-region, the corresponding regions after registration are formed into an overall surface for analysis. It can be seen from Figure 12a that the entire surface formed by each region have a good overall fit, and there is no overlapping of each sub-region and no deformation of the entire surface. It can be seen from Figure 12b that due to point clouds having been filtered through differential geometric properties, the overall similar surfaces can be well fitted where the curvature changes and distortions are large, and the corresponding points can be accurately matched. There is no situation that the overall similar surfaces are still difficult to coincide after registration as in Figure 5. Therefore, the geometric transformation relationship $M = \{m_1, m_2, m_3, \ldots, m_{20}\}$

between the overall similar surfaces can be composed of the transformation relationship m_i of each sub-region. This proves that the method of region registration in this paper can effectively solve the overall spatial transformation relationship of similar surfaces with complex transformations.

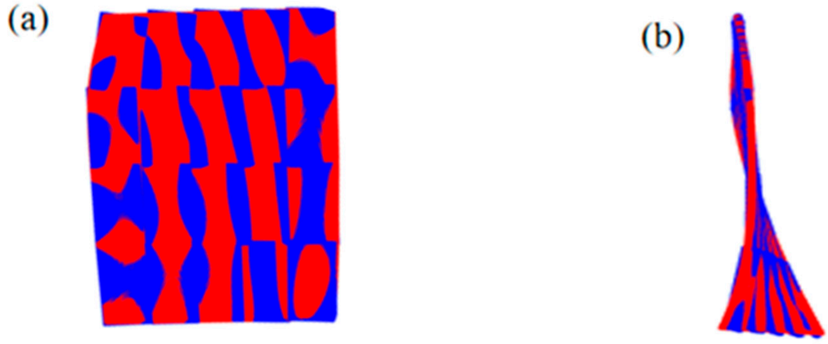

Figure 12. The overall registration effect of each sub-region: (**a**) front view of overall similar surface, (**b**) side view of overall similar surface.

5. Conclusions

A method for solving the spatial transformation relationship of similar ruled surfaces is proposed based on registration of divided regions in this paper, which can solve the geometric transformation relationship between similar surfaces with complex flexible transformations such as local deformation or curvature changes. The main contributions can be summarized as follows:

1. An adaptive region division algorithm is proposed to accurately divide the complex surfaces by finding curvature mutation points on the surface boundary. This region division algorithm can ensure that the corresponding regions between similar surfaces are similar in shape, and have the same number, which provides the possibility for the subsequent point cloud registration of each sub-region.
2. The traditional S-ICP algorithm is improved by introducing the similarity judgment of curvature characteristics and differential geometry properties, and the registration efficiency and accuracy are improved. Moreover, the improved S-ICP algorithm can ensure that the differential geometric properties between corresponding points are similar after registration, which provides a basis for mapping and reuse of process knowledge between corresponding points on similar surfaces.
3. The calculation results show that the method proposed in this paper can effectively complete the registration of each sub-region and solve the spatial transformation relationship. Compared with the traditional S-ICP algorithm, the registration accuracy of the proposed method is improved, and the registration time of each sub-region is reduced by about 20%. In addition, the simulation results show that the registration effect of the overall surface which is formed by each sub-region after registration is also very good, it can achieve a better fit even in the area of local deformation or curvature changes. It is proven that the proposed method in this paper is suitable for the situation that it is difficult to solve the spatial geometric transformation relationship of similar surfaces with complex transformation through global registration.

However, the method in this paper cannot solve the numerical value of curvature change and torque deformation between similar surfaces, and when the degree of curvature changes or torque deformation between similar surfaces is too large, it is difficult to achieve accuracy in the final registration result, so it is also an important research direction of our future work.

Author Contributions: F.H. and Z.H. conceptualized the study. F.H. drew up the paper direction and solution. Z.H. compiled the algorithm and completed the simulation experiment. L.H. corrected the point cloud data. X.P. analyzed and corrected the data error. M.Y. and C.Z. supplied significant information regarding the current research to the introduction and conclusion. All authors have read and agreed to the published version of the manuscript.

Funding: This work was supported by the National Natural Science Foundation of China (51905418), the Coal Joint Fund Project of Shaanxi (2019JLM-37), the Excellent Youth Fund of Xi'an University of Science and Technology(2020YQ3-07), and the Opening Topic Fund of Key Laboratory of Aeroengine High Performance Manufacturing Industry and Information Technology of Ministry of China (HPM-2020-04). Shaanxi innovative talents promotion plan—Science and technology innovation team (2021TD-27).

Institutional Review Board Statement: Not applicable.

Informed Consent Statement: Not applicable.

Data Availability Statement: Not applicable.

Conflicts of Interest: The authors declare no conflict of interest.

References

1. Huang, R.; Zhang, S.; Xu, C.; Zhang, X.; Zhang, C. A flexible and effective NC machining process reuse approach for similar subparts. *Comput. -Aided Des.* **2015**, *62*, 64–77. [CrossRef]
2. Huang, B.; Zhang, S.; Huang, R.; Li, X.; Zhang, Y. An effective retrieval approach of 3D CAD models for macro process reuse. *Int. J. Adv. Manuf. Technol.* **2019**, *102*, 1067–1089. [CrossRef]
3. Sun, Y.; Jia, J.; Xu, J.; Chen, M.; Niu, J.P. feedrate and trajectory planning for free-form surface machining: A state-of-the-art review. *Chin. J. Aeronaut.* **2022**, *35*, 12–29. [CrossRef]
4. Yan, S.; Sun, Y. Early chatter detection in thin-walled workpiece milling process based on multi-synchro squeezing transform and feature selection. *Mech. Syst. Signal Process* **2022**, *169*, 108622. [CrossRef]
5. Sun, Y.; Jiang, S. Predictive modeling of chatter stability considering force-induced deformation effect in milling thin-walled parts. *Int. J. Mach. Tools Manuf.* **2018**, *135*, 38–52. [CrossRef]
6. Huang, R.; Jing, J.F.; He, K.; Chen, Z. An effective free form surface retrieval approach for potential machining process reuse. *Int. J. Adv. Manuf. Technol.* **2017**, *91*, 4341–4358. [CrossRef]
7. Thompson, E.H. An exact linear solution of the problem of absolute orientation. *Photogrammetria* **1958**, *15*, 163–179. [CrossRef]
8. Horn, B.K.P. Closed-form solution of absolute orientation using unit quaternions. *J. Opt. Soc. Am. A* **1987**, *4*, 629–642. [CrossRef]
9. Besl, P.J.; Mckay, H.D. A method for registration of 3-D shapes. *IEEE Trans. Pattern Anal. Mach. Intell.* **1992**, *14*, 239–256. [CrossRef]
10. Yao, Z.; Zhao, Q.; Li, X.; Bi, Q. Point cloud registration algorithm based on curvature feature similarity. *Measurement* **2021**, *177*, 109274. [CrossRef]
11. Xu, G.; Pang, Y.; Bai, Z.; Wang, Y.; Lu, Z. A Fast Point Clouds Registration Algorithm for Laser Scanners. *Appl. Sci.* **2021**, *11*, 3426. [CrossRef]
12. Žagar, B.L.; Yurtsever, E.; Peters, A.; Knoll, A.C. Point Cloud Registration With Object-Centric Alignment. *IEEE Access* **2022**, *10*, 76586–76595. [CrossRef]
13. Geng, N.; Ma, F.; Yang, H.; Li, B.; Zhang, Z. Neighboring constraint-based pairwise point cloud registration algorithm. *Multimed. Tools Appl.* **2016**, *75*, 16763–16780. [CrossRef]
14. Lu, J.; Wang, Z.; Hua, B.; Chen, K. Automatic point cloud registration algorithm based on the feature histogram of local surface. *PLoS ONE* **2020**, *15*, e0238802. [CrossRef]
15. Li, J.; Huang, S.; Cui, H.; Ma, Y.; Chen, X. Automatic Point Cloud Registration for Large Outdoor Scenes Using a Priori Semantic Information. *Remote Sens.* **2021**, *13*, 3474. [CrossRef]
16. Du, S.Y.; Zheng, N.; Lei, X.; Ying, S.H.; Xue, J. Scaling iterative closest point algorithm for registration of m-D point sets. *J. Vis. Commun. ImageRepresentation* **2010**, *21*, 442–452. [CrossRef]
17. Wang, C.; Shu, Q.; Yang, Y.; Deng, S. Point cloud registration in multidirectional affine transformation with variance compensation. *Acta Opt. Sin.* **2019**, *39*, 0215002. [CrossRef]
18. Shu, Q.; He, X.; Wang, C.; Yang, Y.; Cui, Z. Fast point cloud registration in multidirectional affine transformation. *Opt. —Int. J. Light Electron Opt.* **2021**, *229*, 165884. [CrossRef]
19. Netto, G.M.; Oliveira, M.M. Robust point-cloud registration based on dense point matching and probabilistic modeling. *Vis Comput.* **2022**, *38*, 3217–3230. [CrossRef]
20. Han, F.Y.; Zhang, C.W.; Guo, W.; Peng, X.L.; Zhang, W. A high-efficiency generation method of integral impeller channel tool path based on parametric domain template trajectory mapping. *Int. J. Adv. Manuf. Technol.* **2019**, *100*, 75–85. [CrossRef]
21. Ying, S.H.; Peng, J.G.; Du, S.Y.; Qiao, H. A Scale Stretch Method Based on ICP for 3D Data Registration. *IEEE Trans. Autom. Sci. Eng.* **2009**, *6*, 559–565. [CrossRef]

22. Zhang, L.; Guo, J.; Xiao, J. Blending Surface Segmentation and Editing for 3D Models. *IEEE Trans. Vis. Comput. Graph.* **2020**, *28*, 2879–2894. [CrossRef] [PubMed]
23. Wan, J.; Li, X. Analysis of a superconvergent recursive moving least squares approximation. *Appl. Math. Lett.* **2022**, *133*, 108223. [CrossRef]
24. Wang, C.; Shu, Q.; Yang, Y.; Deng, S. Point Cloud Registration in Multidirectional Affine Transformation. *IEEE Photonics J.* **2018**, *10*, 1–15. [CrossRef]
25. Barequet, G.; Sharir, M. Partial Surface and Volume Matching in Three Dimensions. *IEEE Trans. Pattern Anal. Mach. Intell.* **1998**, *19*, 929–948. [CrossRef]
26. Li, L.; Cao, X.; Sun, J. Three-Dimensional Point Cloud Registration Based on Normal Vector Angle. *J. Indian Soc. Remote Sens.* **2019**, *47*, 585–593. [CrossRef]